Hindawi Publishing Corporation
ISRN Analytical Chemistry
Volume 2014, Article ID 391836, 8 pages
http://dx.doi.org/10.1155/2014/391836

Research Article

Altered Metabolic Profile in Congenital Lung Lesions Revealed by ^{1}H Nuclear Magnetic Resonance Spectroscopy

Maria Chiara Mimmi,[1] Maurizio Ballico,[1] Ghassan Nakib,[2] Valeria Calcaterra,[3] Jose Louis Peiro,[4] Mario Marotta,[5] and Gloria Pelizzo[2]

[1] *Department of Medical and Biological Sciences, University of Udine, Piazzale M. Kolbe 4, 33100 Udine, Italy*
[2] *Department of the Mother and Child Health, Pediatric Surgery Unit, IRCCS Policlinico San Matteo Foundation Pavia and University of Pavia, 27100 Pavia, Italy*
[3] *Department of the Mother and Child Health, Pediatric Unit, IRCCS Policlinico San Matteo Foundation Pavia and Department of Internal Medicine, University of Pavia, 27100 Pavia, Italy*
[4] *Pediatric Surgery, Orthopaedics and Bioengineering Laboratory, Research Institute, Vall d'Hebron University Hospital, 08035 Barcelona, Spain*
[5] *Pediatric Surgery, Fetal Program, Vall d'Hebron University Hospital, 08035 Barcelona, Spain*

Correspondence should be addressed to Maria Chiara Mimmi; chiara.mimmi@uniud.it

Received 11 November 2013; Accepted 17 December 2013; Published 29 January 2014

Academic Editors: T. Fossen and I. Zhukov

Congenital lung lesions are highly complex with respect to pathogenesis and treatment. Large-scale analytical methods, like metabolomics, are now available to identify biomarkers of pathological phenotypes and to facilitate clinical management. Nuclear magnetic resonance (NMR) is a unique tool for translational research, as *in vitro* results can be potentially translated into *in vivo* magnetic resonance protocols. Three surgical biopsies, from congenital lung malformations, were analyzed in comparison with one control sample. Extracted hydrophilic metabolites were submitted to high resolution ^{1}H NMR spectroscopy and the relative concentration of 12 metabolites was estimated. In addition, two-dimensional NMR measurements were performed to complement the results obtained from standard monodimensional experiments. This is one of the first reports of *in vitro* metabolic profiling of congenital lung malformation. Preliminary data on a small set of samples highlights some altered metabolic ratios, dealing with the glucose conversion to lactate, to the relative concentration of phosphatidylcholine precursors, and to the presence of myoinositol. Interestingly some relations between congenital lung lesions and cancer metabolic alterations are found.

1. Introduction

Lung development is a highly regulated and coordinated process, typified by stage specific changes in structure and function, which includes branching morphogenesis, angiogenesis, sacculation, alveologenesis, and cytodifferentiation [1]. Congenital pulmonary disease is characterized by a wide variety of abnormalities arising at different stages of the process [2].

Metabolomics is an emerging approach that uses analytical techniques, such as nuclear magnetic resonance (NMR) [3] spectroscopy, or mass spectrometry (MS) [4], to achieve a comprehensive global monitoring of metabolites and their fluctuations in response to various stimuli.

Although gene/protein expressions schemes provide useful clues to organs development and function, many factors like posttranslational modifications, alternative gene functions, or compartmentalization also raise important biochemical changes. Therefore, metabolic profiling is essential to completely describe the physiopathological state of a biological system.

Considerable efforts in this sense were devoted to human lung cancer [5, 6] and to human lung injury [7], but very limited information is available about metabolic perturbations arising *in situ* from congenital lung malformations.

The purpose of this study was to determine the feasibility of tissue extraction and analysis of the main hydrosoluble

Table 1: Specimens features summary.

Specimen	Patient	Type of malformation	Sex of patient	Age at surgery	Surgical procedure
N. 1	A	Bronchogenic cyst	M	4 months	Lobectomy
N. 2	B	Congenital lobar emphysema	M	6 months	Lobectomy
N. 3	B	Bronchopulmonary sequestration	M	6 months	Lobectomy
N. 4	C	Control lung	M	7 days	Lung biopsy

metabolites of lung lesions biopsies from human. Three types of congenital malformation were evaluated in comparison to a control lung tissue.

Particular attention was paid to the lactate/glucose (Lac/Glc) ratio and to choline (Cho) compounds, which are involved in the phosphatidylcholine (PtdCho) synthesis and catabolism.

Many reasons lead us to focus on these particular metabolic pathways; first of all a hyperactive glycolysis as well as the following increment of the Lac/Glc ratio is associated with lung inflammatory state [7] and represents, for instance, a diagnostic tool related to lung cancers [5, 6].

The principal argument to investigate PtdCho metabolism, which actually include choline and glucose, is the crucial role of this phospholipid as the main component of alveolar surfactant [8].

Many data prove that a disturbed surfactant metabolism plays a role in several neonatal lung diseases, such as congenital diaphragmatic hernia (CDH) [9]. A further prompt to focus on glucose and choline pathways comes from the results of Raman mapping and FTIR imaging studies on congenital pulmonary airways malformations (CPAM), in which an accumulation of PtdCho and glycogen was noted [10].

In addition, it is generally accepted that the cycle of PtdCho, the major phospholipid component of eukaryotic cells, is affected by malignant proliferations; free choline and its derivatives phosphocholine (PCho) and glycerophosphocholine GPCho represent relevant biomarkers for diagnostic and therapeutic tools [11].

Finally, NMR spectroscopy is a unique tool for translational research. NMR-based metabolomics can provide a comprehensive information on the degree of organ dysfunction and the metabolic biomarkers discovered *in vitro* can be translated into *in vivo* magnetic resonance spectroscopy protocols.

2. Materials and Methods

2.1. Instrumentation and Reagents. ^{1}H NMR experiments were acquired on a Bruker Avance spectrometer operating at 500 MHz (Bruker BioSpin, Germany).

Tissue homogenization was performed by Ultra Turrax T25 Homogenizer (IKA, Germany). Water was ultrapure (mQ H_2O) and solvents were of HPLC grade (Sigma Aldrich, United States).

2.2. Tissue Extraction. Three biopsies were obtained from pathological lung tissue of two infants who underwent surgery for congenital malformations. The control biopsy was from a newborn deceased on the 7th day of life. The samples were immediately frozen in liquid nitrogen after collection and stored at −80°C. In Table 1 the characteristics of the tissue sections are reported.

The frozen biopsies were put in plastic test tube and kept dipped into liquid nitrogen during the homogenization process. While samples N. 2, N. 3, and N. 4 were completely pulverized in ca 5 minutes, sample N. 1 proved resistant to homogenization and a nucleus of tissue remained intact. The specimens weight after homogenization ranged roughly between 30 and 110 mg. Immediately after weighting, a biphasic extraction of metabolites was performed, following a previously reported protocol [12]. The obtained dry extracts were stored at −80°C until NMR analysis.

2.3. NMR Spectroscopy

2.3.1. Data Acquisition. An aliquot of each aqueous extract (corresponding to 30–50 mg of frozen pulverized tissue) was redissolved in 0.65 mL of deuterated phosphate buffer at pH 7.4, containing Na_2HPO_4/NaH_2PO_4 50 mM, TSP^-Na^+-d_4 (sodium 3-trimethyl-silyl [2,2 3,3-d_4] propionate) 0.1 mM as a frequency reference, and NaN_3 0.5 mM to prevent bacterial growth. The working temperature was 298 K.

Standard monodimensional ^{1}H spectra included flip-angle pulses of 30° and residual solvent suppression by presaturation applied during the 5 s relaxation delay.

Two-dimensional TOCSY [13] spectra were also acquired and the acquisition scheme *mlevphpr* [14] included solvent suppression by presaturation [15], applied along the 2 s relaxation delay, and mixing time of 80 ms.

Spectra acquisition and processing were performed with the Bruker software TOPSPIN.

2.3.2. Data Treatment. After FID apodization with a line broadening window function, all 1D spectra were phased, Fourier-transformed, and chemical-shift referenced. The signals overlapping made the direct integration of peaks area impossible; therefore, a spectrum modeling (peak fitting) was performed with ACD/Labs 10. The experimental spectrum was divided in regions containing not more than 100 peaks prior to modeling with a combination of Gauss and Lorentz functions.

For the relative quantification of the metabolites of interest each fitted integral was normalized versus the total area of the spectrum and corrected for the numbers of protons associated to the assigned peak. The normalization permitted overcoming the differences in biopsies dimensions and homogenization and allowed for a comparison of metabolites levels among pathological and control tissues.

The error associated with each modeled peak integral was calculated by the following formula:

$$\text{Error}_{\text{Modeled Peak Integral}} = \text{Modeled Peak Integral} \times \frac{\sqrt{\text{Total RSS}}}{\text{Total Integral}}, \quad (1)$$

where Total RSS stands for residual sum of squared differences between the calculated spectrum and original experimental data, while Total Integral stands for the absolute integral of the spectral region used for fitting and RSS determination.

Only a small region of 2D TOCSY spectra (in the range 3.0–4.6 ppm) was used to evaluate the relative concentration of free Cho and its derivatives PCho and GPCho; the diagnostic cross peaks of the three compounds are generated by the two methylene groups adjacent to the quaternary ammonium (see Figure 1). The height of significant cross peaks was measured with the software Sparky (NMR Assignment and Integration software) and the noise was taken as confidence limit of the measure. The noise was estimated as the median of 30 randomly sampled absolute value data heights.

3. Results

The ^{1}H-1D NMR analysis of aqueous extracts from surgical biopsies provided an overview of the main hydrosoluble metabolites. The relative concentration of the assigned metabolites was obtained by normalizing each integral value, corrected for the proton number, versus the total area of the spectrum and is shown in Table 2 and Figure 2.

The most important differences of malformation tissues versus control lung regarded the ratio lactic acid/glucose or Lac/Glc (here intended as Lac/β-D-glucose) (Table 3). This parameter, that reflects an enhanced glycolysis to produce lactic acid, was particularly high in bronchopulmonary sequestration and to a lesser extent in congenital lobar emphysema, compared to the control lung and bronchogenic cyst samples.

The other metabolite that discriminated pathological from healthy tissue was myoinositol whose level was lower in the control lung compared to the three malformation samples.

Among the assigned compounds, the phosphatidylcholine precursors were included (namely, Cho, PCho, and GPCho). In the adopted pH conditions the diagnostic peaks of choline compounds, arising from the methyl groups of the quaternary ammonium, were in the range 3.20–3.25 ppm; this resulted to be a very crowded region where also glucose and other compounds resonances were detected (Figure 3). In particular PCho and GPCho could not be measured in the control lung due to the overlapping of glucose signals that was particularly concentrated in this sample. For the same reason GPCho could not be determined in the bronchogenic cyst tissue.

Apart from the mentioned inconvenience, the 1D NMR analysis showed some remarkable variations. The level of the free Cho decreased with the following order: congenital lobar emphysema, bronchogenic cyst, bronchopulmonary sequestration, control lung. The level of PCho decreased with the following order: congenital lobar emphysema, bronchogenic cyst, bronchopulmonary sequestration (control lung not determined). The relative concentration of GPCho was noted to be higher in congenital lobar emphysema than in bronchopulmonary sequestration.

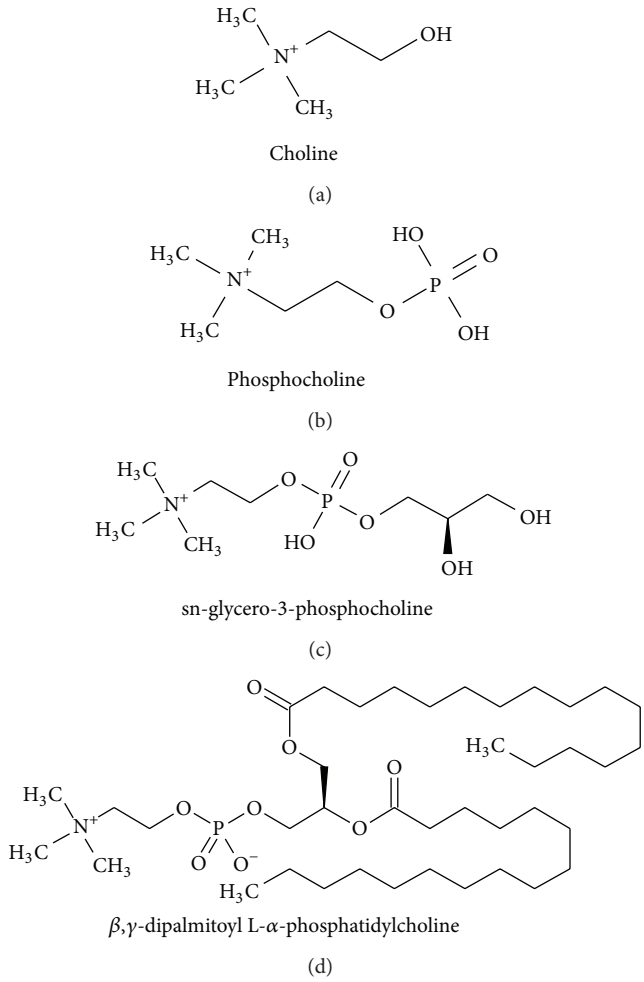

Figure 1: Chemical structure of choline, phosphocholine, sn-glycero-3-phosphocholine, and β,γ-dipalmitoyl-L-α-phosphatidylcholine (principal component of pulmonary surfactant).

The limits of 1D NMR analysis prompted us to exploit 2D NMR TOCSY experiments to estimate the Cho compounds level. Although the correlation of metabolite concentration with TOCSY peaks intensity is not linear, it has been proved that the variation of choline compounds signals reflects their concentration difference [16] (Figure 4).

To overcome the inhomogeneity among biopsies dimensions, and consequently of global spectra intensity, we focused on the relative peaks intensity instead of comparing their absolute values. In Table 3, we reported the ratio of PCho and GPCho cross peak height; this ratio decreased with the following order: congenital lobar emphysema, bronchopulmonary sequestration, bronchogenic cyst, control lung. Unfortunately, the cross peak of free Cho could not be taken

Table 2: Results of ^{1}H 1D NMR analysis of aqueous extracts from lung tissue specimens. The relative concentration of metabolites is expressed as percentage fraction of the peak integral over the total spectrum integral. Each peak integral (singlet or multiplet) is obtained by curve fitting and is corrected for the number of protons. The confidence limits are calculated from fitting residual (see Materials and Methods section, Equation (1)). In some cases more than one peak for metabolite is unequivocally assigned; therefore, the associated concentration values are reported.

Metabolite	Broncho pulmonary sequestration (% fraction of total spectrum area)	Bronchogenic cyst (% fraction of total spectrum area)	Congenital lobar emphysema (% fraction of total spectrum area)	Control lung (% fraction of total spectrum area)
Lactic acid	2.71 ± 0.02	3.09 ± 0.02	3.40 ± 0.02	4.42 ± 0.04
Alanine	0.402 ± 0.003	0.458 ± 0.003	0.806 ± 0.005	0.319 ± 0.003
Glutamic acid	0.576 ± 0.005	0.798 ± 0.005	1.093 ± 0.007	0.620 ± 0.006
Succinic acid	0.0721 ± 0.0006	0.0504 ± 0.0003	0.0349 ± 0.0002	0.189 ± 0.002
Creatine	0.1498 ± 0.0008	0.260 ± 0.001	0.1788 ± 0.0009	0.182 ± 0.001
Choline	0.0768 ± 0.0004	0.1079 ± 0.0005	0.279 ± 0.001	0.0718 ± 0.0004
Phosphocholine	0.0827 ± 0.0005	0.1063 ± 0.0005	0.1883 ± 0.0009	ND
Glycerophosphocholine	0.0744 ± 0.0004	ND	0.1145 ± 0.0006	ND
Glucose beta	0.0433 ± 0.0002	0.790 ± 0.004	0.324 ± 0.002	1.143 ± 0.007
Myoinositol	1.019 ± 0.006	1.137 ± 0.005	1.364 ± 0.007	0.522 ± 0.003
Creatine	0.192 ± 0.001	0.311 ± 0.001	0.223 ± 0.001	0.170 ± 0.001
Myoinositol_b	0.847 ± 0.005	1.371 ± 0.007	1.932 ± 0.009	0.472 ± 0.003
Formic acid	1.5 ± 0.1	0.23 ± 0.02	0.10 ± 0.01	0.42 ± 0.02

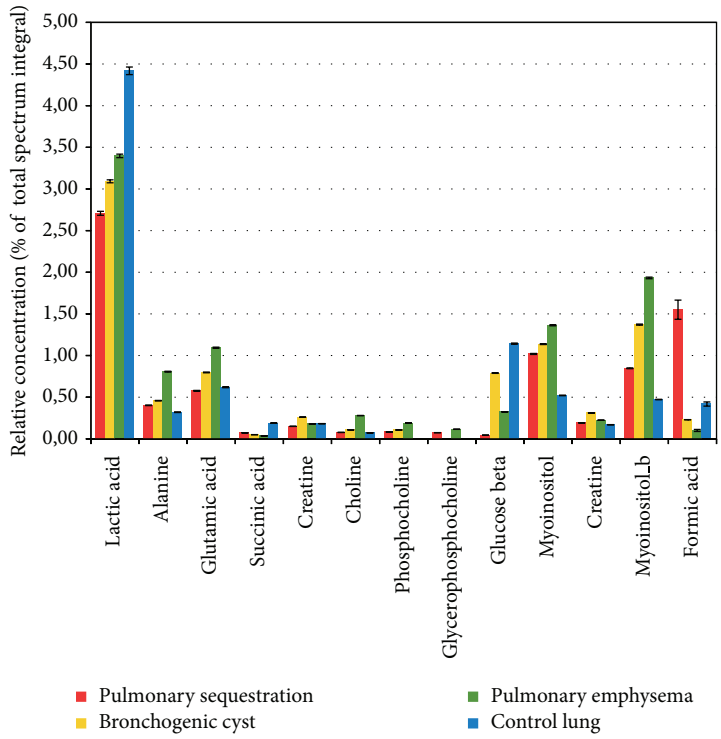

Figure 2: Bar diagram representation of data reported in Table 2. Phosphocholine is not detected in control lung spectrum (concentration below detection limit). Glycerophosphocholine cannot be observed in bronchogenic cyst and in control lung spectra, due to the overlapping of glucose whose level is particularly high in the two samples.

Table 3: Metabolites ratio in lung neonatal tissues. The first three ratios are obtained by ^{1}H 1D NMR results reported in Table 2. The PCho/GPCho ratio is derived from ^{1}H-^{1}H 2D NMR analysis: diagnostic cross peak heights of PCho and GPCho are compared to give a semiquantitative estimate of their relative concentration. Ratios and associated confidence limits are derived as reported in Experimental Section.

Metabolites ratio	Broncho pulmonary sequestration	Bronchogenic cyst	Congenital lobar emphysema	Control lung
	1D NMR	1D NMR	1D NMR	1D NMR
Lac/Glc	62.5 ± 0.5	3.91 ± 0.02	10.48 ± 0.07	3.87 ± 0.04
Lac/Creat	18.1 ± 0.2	11.9 ± 0.07	19.0 ± 0.1	24.2 ± 0.2
Myo/Glc	23.5 ± 0.1	1.44 ± 0.01	4.21 ± 0.02	0.457 ± 0.003
	2D NMR	2D NMR	2D NMR	2D NMR
PCho/GPCho	5.6 ± 0.5	0.96 ± 0.04	7.0 ± 0.2	0.41 ± 0.02

into consideration because of overlapping with one of the myoinositol cross peaks (Figure 4).

We observed that GPCho is clearly more concentrated in the control lung than in malformations, while on the contrary PCho level is higher in malformations than in control lung, as it comes out from the qualitative observation of TOCSY maps.

4. Discussion

The lung is a complex organ consisting of more than 40 distinct cell types derived from ectodermal, mesenchymal, and endodermal compartments with a number of specialized functions related to gas exchange, host defense, and ion transport [17].

The spectrum of congenital lung lesions likely results from disordered embryologic interactions, occurring during the course of fetal lung development. Bronchopulmonary sequestrations are microscopic cystic masses of nonfunctioning pulmonary, which have a blood supply originating from the aorta rather than the pulmonary artery, and an absence of communication with the bronchial tree. BPS is likely to arise between the 4th and 8th week gestation during the pseudoglandular period. Also most bronchogenic cysts develop during this phase and it result from abnormal budding of the foregut. congenital lobar emphysema usually develops during the canalicular stage (16–26 weeks gestation) and it is an overinflation and distension of one or more pulmonary lobes, possibly secondary to a defect in the bronchial cartilage.

A detailed understanding of the biochemical processes governing stage specific changes during lung maturation and the eventual lesion onset is still lacking. Describing physiopathological lung development, at a molecular resolution, could lead to new perspectives in treatment of congenital

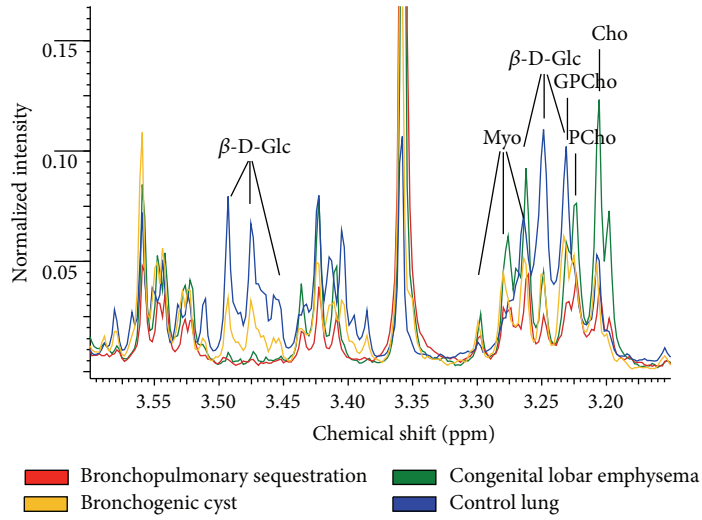

FIGURE 3: Selected region of 500 MHz ^{1}H 1D NMR spectra of tissues extracts. Different colors are used to distinguish different samples traces. Attribution of signals arising from free choline, choline phosphorylated derivatives, myoinositol, and β-D-glucose are shown.

malformations either in prenatal or in postnatal period. Tissue characterization of pulmonary malformation in infants and children could be useful with the perspective to give valuable information about lung maturation, timing, lung repair, and regeneration.

The aim of the this work was establishing a protocol for the extraction of hydrophilic metabolites from lung tissues, as well as for their quantification by NMR, prior to embarking on a large scale study to identify biomarkers of congenital lesions.

The first challenge we met was related to the intrinsic limitations of 1D NMR spectroscopy applied to a complex mixture of unfractionated compounds as in the case of any biological tissue extracts. The signals superposition was overcome by peak fitting, and in addition 2D NMR spectroscopy was exploited to get a semiquantitative estimate of Cho derivatives concentrations.

Though being aware that biomarkers identification must build on a statistically significant set of samples, we could make some interesting observations that regarded, first of all, the ratio Lac/Glc. An enhanced Glc utilization, a hallmark of malignant transformation, was observed for pulmonary sequestration and to a lesser extent for pulmonary emphysema, while the level of bronchogenic cyst was very similar to the control lung (Table 3).

It must be said that both Lac and Glc were higher in the bronchogenic cyst and in the control samples than in the remaining two samples. The investigation of a more numerous sample will clarify this variability.

From the analysis of 1D NMR data it resulted as well that myoinositol (Myo) accumulated in malformation tissues compared to the control lung; interestingly the Myo level decreased in the order pulmonary sequestration, pulmonary emphysema, bronchogenic cyst, with the latter very similar to the control lung. This evidence could be worthy of further investigation, if it was considered that myoinositol is involved in fetal lung maturation as reported by Fanos et al. [18].

The last remarkable finding, which seemed to discriminate the normal lung from malformations, was based on 2D NMR analysis and regarded the ratio of PCho/GPCho cross peak height; this ratio decreased with the following order: pulmonary emphysema, pulmonary sequestration, bronchogenic cyst, control lung. Again, the last two samples were more homogeneous than the first two conditions. Interestingly, there seems to be a link between the reported observations and what is already known in the field of cancer research. It is generally accepted, in fact, that the cycle of PtdCho, the major phospholipid component of eukaryotic cells, is affected by malignant proliferations [11]. This causes an alteration of PCho and GPCho levels which can be detected by high resolution NMR; in particular an elevated size of PCho generally reflects a high rate of cell proliferation, while the spectral parameter PCho/GPCho has the role of malignancy indicator in cancer [19].

5. Conclusions

The comprehension of biological mechanisms and timing related to congenital lung malformations is still incomplete. Numerous studies and clinical trials have focused on the role of surfactant in lung maturation and function; much attention has been devoted also to the effect of surfactant deficiency in preterm infants and in neonatal lung diseases. In spite of that, a more detailed picture of the biochemical pathways involved in lung lesions onset during pregnancy could have positive outcomes both on diagnostic and therapeutic strategies of pediatric management.

To the best of our knowledge this is one of the first applications of metabolomics to human tissues derived from congenital lung lesions.

Although limited to a small set of samples this study highlights some altered metabolic ratios, dealing with the glucose conversion to lactate, to the relative concentration of PtdCho

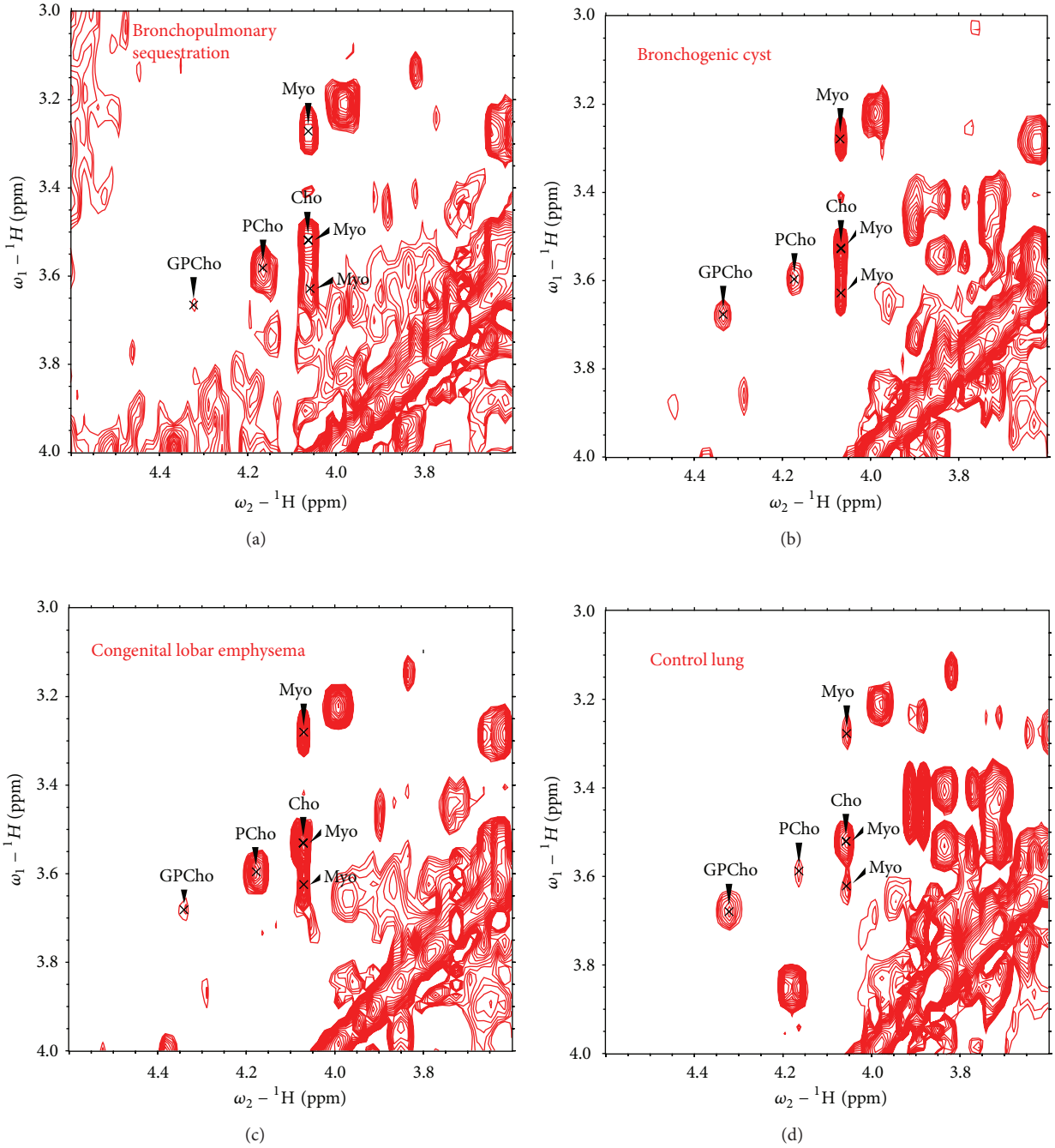

FIGURE 4: Selected region from 500 MHz TOCSY NMR spectra of tissues aqueous extracts. The cross peaks arising from free choline, choline phosphorylated derivatives, and myoinositol are marked and labeled.

hydrosoluble precursors and to the presence of myoinositol. Interestingly, some unexpected relations between congenital lung lesions and cancer metabolic alterations are found.

Further investigation of the regulation of these metabolic traits can have a manifold outcome: first of all, the translation of *in vitro* NMR findings to *in vivo* MRS (Magnetic Resonance Spectroscopy) diagnosis of fetal lung maturity and development.

List of Abbreviations

NMR: Nuclear magnetic resonance
MS: Mass spectrometry
Lac: Lactate
Glc: Glucose
Cho: Choline
PtdCho: Phosphatidylcholine
CDH: Congenital diaphragmatic hernia

CPAM: Congenital pulmonary airways malformations
PCho: Phosphocholine
GPCho: Glycerophosphocholine
TOCSY: Total correlation spectroscopy.

Conflict of Interests

The authors declare that there is no conflict of interests regarding the publication of this paper.

Acknowledgments

This work was financially supported by the Italian Ministry for University and Research (FIRB 2010 RBFR109EOS). The authors wish to thank Dr. F. Combi for collaborating in collecting research samples.

References

[1] D. Warburton, M. Schwarz, D. Tefft, G. Flores-Delgado, K. D. Anderson, and W. V. Cardoso, "The molecular basis of lung morphogenesis," *Mechanisms of Development*, vol. 92, no. 1, pp. 55–81, 2000.

[2] T. Berrocal, C. Madrid, S. Novo, J. Gutiérrez, A. Arjonilla, and N. Gómez-León, "Congenital anomalies of the tracheobronchial tree, lung, and mediastinum: embryology, radiology, and pathology," *Radiographics*, vol. 24, no. 1, article e17, 2004.

[3] O. Beckonert, H. C. Keun, T. M. D. Ebbels et al., "Metabolic profiling, metabolomic and metabonomic procedures for NMR spectroscopy of urine, plasma, serum and tissue extracts," *Nature Protocols*, vol. 2, no. 11, pp. 2692–2703, 2007.

[4] W. Lu, B. D. Bennett, and J. D. Rabinowitz, "Analytical strategies for LC-MS-based targeted metabolomics," *Journal of Chromatography B*, vol. 871, no. 2, pp. 236–242, 2008.

[5] T. W. M. Fan, A. N. Lane, R. M. Higashi et al., "Altered regulation of metabolic pathways in human lung cancer discerned by ^{13}C stable isotope-resolved metabolomics (SIRM)," *Molecular Cancer*, vol. 8, article 41, 2009.

[6] K. Kami, T. Fujimori, H. Sato et al., "Metabolomic profiling of lung and prostate tumor tissues by capillary electrophoresis time-of-flight mass spectrometry," *Metabolomics*, vol. 9, no. 2, pp. 444–453, 2013.

[7] N. J. Serkova, Z. van Rheen, M. Tobias, J. E. Pitzer, J. E. Wilkinson, and K. A. Stringer, "Utility of magnetic resonance imaging and nuclear magnetic resonance-based metabolomics for quantification of inflammatory lung injury," *American Journal of Physiology*, vol. 295, no. 1, pp. L152–L161, 2008.

[8] L. J. I. Zimmermann, D. J. M. T. Janssen, D. Tibboel, A. Hamvas, and V. P. Carnielli, "Surfactant metabolism in the neonate," *Biology of the Neonate*, vol. 87, no. 4, pp. 296–307, 2005.

[9] A. Akella and S. B. Deshpande, "Pulmonary surfactants and their role in pathophysiology of lung disorders," *Indian Journal of Experimental Biology*, vol. 51, no. 1, pp. 5–22, 2013.

[10] C. Krafft, D. Codrich, G. Pelizzo, and V. Sergo, "Raman mapping and FTIR imaging of lung tissue: congenital cystic adenomatoid malformation," *Analyst*, vol. 133, no. 3, pp. 361–371, 2008.

[11] K. Glunde, Z. M. Bhujwalla, and S. M. Ronen, "Choline metabolism in malignant transformation," *Nature Reviews Cancer*, vol. 11, no. 12, pp. 835–848, 2011.

[12] M. C. Mimmi, P. Picotti, A. Corazza et al., "High-performance metabolic marker assessment in breast cancer tissue by mass spectrometry," *Clinical Chemistry and Laboratory Medicine*, vol. 49, no. 2, pp. 317–324, 2011.

[13] L. Braunschweiler and R. R. Ernst, "Coherence transfer by isotropic mixing: application to proton correlation spectroscopy," *Journal of Magnetic Resonance*, vol. 53, no. 3, pp. 521–528, 1983.

[14] A. Bax and D. G. Davis, "MLEV-17-based two-dimensional homonuclear magnetization transfer spectroscopy," *Journal of Magnetic Resonance*, vol. 65, no. 2, pp. 355–360, 1985.

[15] D. I. Hoult, "Solvent peak saturation with single phase and quadrature fourier transformation," *Journal of Magnetic Resonance*, vol. 21, no. 2, pp. 337–347, 1976.

[16] D. Morvan, A. Demidem, J. Papon, and J. C. Madelmont, "Quantitative HRMAS proton total correlation spectroscopy applied to cultured melanoma cells treated by chloroethyl nitrosourea: demonstration of phospholipid metabolism alterations," *Magnetic Resonance in Medicine*, vol. 49, no. 2, pp. 241–248, 2003.

[17] Y. Xu, Y. Wang, V. Besnard et al., "Transcriptional programs controlling perinatal lung maturation," *PLoS ONE*, vol. 7, no. 8, Article ID e37046, 2012.

[18] V. Fanos, L. Atzori, K. Makarenko, G. B. Melis, and E. Ferrazzi, "Metabolomics application in maternal-fetal medicine," *BioMed Research International*, vol. 2013, Article ID 720514, 9 pages, 2013.

[19] F. Podo, "Tumour phospholipid metabolism," *NMR in Biomedicine*, vol. 12, no. 7, pp. 413–439, 1999.